Available online at www.sciencedirect.com
ScienceDirect
Optics Communications 281 (2008) 2139–2144
OPTICS COMMUNICATIONS
www.elsevier.com/locate/optcom

Light driven self-drilling in glasses

B.P. Antonyuk [a,*], A.Z. Obidin [b], S.K. Vartapetov [b], K.E. Lapshin [b]

[a] Institute of Spectroscopy, Russian Academy of Science, 142190 Troitsk, Moscow Region, Russia
[b] Physics Instrumentation Center, General Physics Institute, Russian Academy of Science, 142190 Troitsk, Moscow Region, Russia

Received 15 August 2007; received in revised form 8 December 2007; accepted 14 December 2007

Abstract

It is shown that ArF laser beam may act as effective driller producing in fuzed quartz micron radius channel up to 1 cm long while diameter of light spot is few millimeters. Drill formation is accompanied by compaction effect in the drill walls therefore material is not thrown out the channel.

PACS: 81.40.T; 42.70.L; 85.60

1. Introduction

Fuzed quartz has unique properties and therefore is widely used as optical material. Its characteristics however reveal temporal change and dependence on various external factors. It is well known compaction effect (increase of density) under fluxes of different nature: X-rays [1,2]; γ-rays [1–6]; ions [1,2]; electrons and neutrons [1,2,7–14] shock waves [15–17]. Compaction effect is accompanied by increase of refractive index $\delta n/n$. Various defects are generated by these fluxes in the glass network resulting in the variation of $\delta n/n$ also. Change of the refractive index causes the undesired abberation of SiO_2 lenses therefore would be studied and controlled.

Influence of laser waves on the material is widely investigated last time [18–43]. Compaction effect and generation of different type of defects are found also under UV and VUV irradiation. Theoretical models are proposed which are in reasonable agreement with the experimental results. Usually light intensity in pulsed laser treatment is given in so called 'laser fluence' units (J/cm^2) being by the definition light energy per cm^2 per pulse. Considerable attention is paid to optical damage experiments at high laser fluence $\approx$10 J/cm^2[15–17,32,43]. We found self-organization effects in fuzed quartz [44,45] at fluences 1–6 J/cm^2 below the damage region. Here we report for the first time about self-drilling effect observed in the region 0.1–1 J/cm^2.

There is direct and obvious way of sample drilling by laser beam when diameter of the produced channel equals to the focused spot size. We are interested here in more subtle and physically rich drilling produced long channel with cross-section much less the spot size. It is not connected with ordinary light induced ablation but is close to crack formation in stressed matter. We shall see that light of moderate power transports electrons in disordered media into long and narrow filaments aligned with wave vector **k**. Strong Coulomb repulsion between the filament walls splits matter producing long drills.

Light driven charged filament formation belongs to the class of self-organization phenomena in open dissipative systems. Typical examples of this class are the Benard convection [46], Belousov–Zhabotinsky reactions [47] and the Turing instability [48]. All self-organization phenomena are driven by some external flow through the system: heat in Benard convection, chemical reagents in Belousov–Zhabotinsky reactions, etc. The optical analogue of Turing instability was presented by Arecchi [49]. In this case light amplitude has been modulated in time and space, which was crucial for the organization to occur. Our investigations

* Corresponding author.
E-mail address: Antonytuk@isan.troitsk.ru (B.P. Antonyuk).

0030-4018/$ - see front matter © 2008 Published by Elsevier B.V.
doi:10.1016/j.optcom.2007.12.033

[50,51] have shown that steady light flow through a system can provide self-organization either.

Electron spectra of a random media consists of extended electron and hole bands divided by the 'gap'. The gap is filled by local states of the electrons trapped in local minima of an electron potential. Electron energy in the trap and trap positions are random. We consider the case when photon energy is less than the gap and light induces electron transitions between local states only. Electrons and holes in extended states are not generated in this conditions. Light driven as well as spontaneous transfers of electrons between the traps are taken into account.

An electron absorbing a photon gains energy and shifts from one trap to another with higher energy level (Fig. 1). For an electron located in initial trap i with the energy level $\varepsilon_i^{(0)}$ there is corresponding absorption band with resonance at some excitation energy M (Fig. 2). The electron can be transported to another trap f with the excitation energy $\varepsilon_{fi} = \varepsilon_f^{(0)} - \varepsilon_i^{(0)}$ within the absorption band and all directions of transfer are equiprobable. Let us denote the transitions with the $\varepsilon_{fi} < M$ as low energy excitations and these with the $\varepsilon_{fi} > M$ as high energy ones. Now we examine light induced electron transition in local electric field $\mathbf{E}$. Field contribution shifts all energy levels hence shifting the excitation energies by $-e\mathbf{R}_{fi}\mathbf{E}$, where $\mathbf{R}_{fi} = \mathbf{R}_f - \mathbf{R}_i$ is vector of the electron transfer, $\mathbf{R}_f$ and $\mathbf{R}_i$ are centers of the final and initial traps respectively:

$$\varepsilon_{fi} = \varepsilon_f^{(0)} - \varepsilon_i^{(0)} - e\mathbf{R}_{fi}\mathbf{E}$$

The directions of transfers are not equivalent any more: all the possible final states that bring electron in opposite direction to the electric force ($\mathbf{R}_{fi}e\mathbf{E} < 0$) get higher excitation energy, among them low energy excitations shift closer to the resonance M (Fig. 2). The final states that would bring the electron in the direction of the electric force reduce the excitation energy and low energy excitations shift off the resonance. That is why low energy transitions of an electron are directed preferably against the acting electric force (in the direction of the potential energy increase). High energy excitations reveal opposite behavior but their life time is less in comparison with deep levels therefore the last dominates in the light driven electron transport. Low energy transitions at high pumping dominate also over ordinary mobility which is quite low in fuzed quartz and independent on laser power.

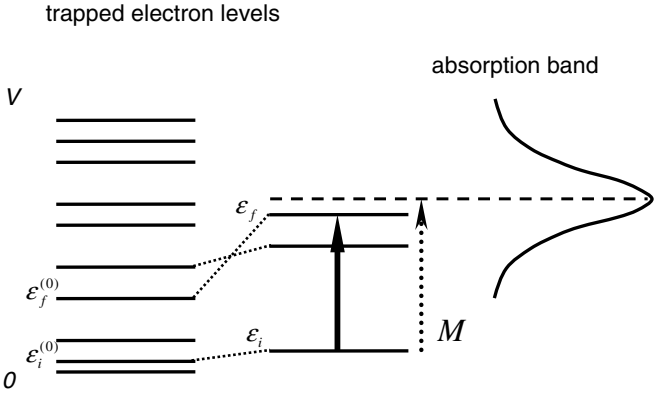

Fig. 2. Light driven electron transitions between trapped levels. Transitions against electric force $e\mathbf{E}$ shift low energy excitations toward the resonance.

2. Charged filaments production and matter splitting under moderate light pumping

Assume light wave vector and polarization are given by vertical arrows $\mathbf{k}$ and horizontal ones $\mathbf{e}$ in Fig. 3 respectively. In general case electron transport from initial trap i to final trap f is possible in any direction with respect to polarization (angle θ_{fi} between radius-vector of transport $\mathbf{R}_f - \mathbf{R}_i$ and polarization $\mathbf{e}$ may be different). Further consideration however shows that if irradiation is not strong enough then during the laser pulse only light driven electron transport in the direction of the light polarization $\mathbf{e}$ is realized ($\theta_{fi} \to 0$). Irradiation with random polarization in the perpendicular to wave vector plain pushes electrons within this plain and against the electric force forming charged filaments. Electrons from the right and left sides

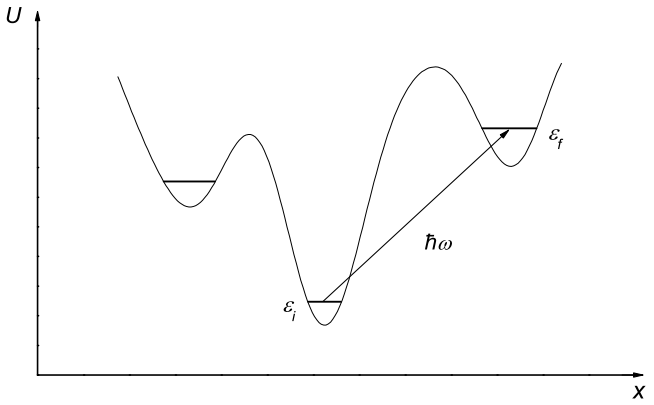

Fig. 1. Light induced electron transfer between different traps in a random medium.

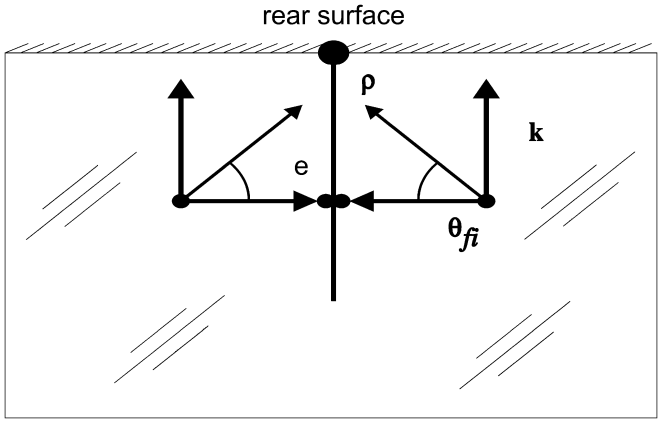

Fig. 3. Electron transport by beam of moderate power: charged filament preparation.

shown in Fig. 3 are transported towards the charged filament aligned with **k**.

The probability rate w_{fi} for light induced electron transition from a trap i to a trap f according to golden rule is

$$w_{fi} \propto |\mathbf{E}\mathbf{d}_{fi}|^2$$

where **E** is electric field of the laser wave and $\mathbf{d}_{fi}$ is dipole moment of the transition:

$$\mathbf{d}_{fi} = \int \varphi_f^*(\mathbf{r} - \mathbf{R}_f) e\mathbf{r} \varphi_i(\mathbf{r}) d^3\mathbf{r}$$

here φ_f and φ_i are the electron wave functions in potential wells f and i respectively, zero of coordinates **r** is taken inside the initial trap i. As far as overlap of wave functions in distant traps is small then integrated functions do not vanish only in small region between the traps f and i therefore $\mathbf{d}_{fi}$ is aligned with $\mathbf{R}_f - \mathbf{R}_i$ and rate w_{fi} becomes dependent on the angle θ_{fi} between light polarization vector and the electron transfer vector $\mathbf{R}_f - \mathbf{R}_i$

$$w_{fi} \propto I\sigma \cos^2\theta_{fi} \exp(-\kappa_{fi}|\mathbf{R}_f - \mathbf{R}_i|) \quad (1)$$

where $I \propto E^2$ is photon flux, σ is cross-section of the process, exponentially decayed with transfer distance factor corresponds to the decay of the wave function outside the traps (see for details [50,51] and pioneering paper [52]).

Polarization of our laser beam is random in the plane perpendicular to the wave vector **k** therefore rate (1) reaches maximum for the electron transport within this plane. If photon flux I is strong enough it compensates small factor $\cos^2\theta_{fi}$ for transfers with $\theta_{fi} \neq 0$ and light induced electron transitions in all directions would be observed. Decrease of pumping makes the angle dependence important hence light of moderate power transports electrons within the plane perpendicular to **k**. According to the presented in Introduction arguments the electron transfer is also in the direction of the potential energy increase (against projection of the acting on the electron electric force $e\mathbf{E}$ on the plane (Fig. 3)). This uncommon transport produces electron bunch ρ on the rear surface where the intensity of the used convergent beam reaches maximum and the bunch will grow against wave vector **k**. So, long charged filaments aligned with **k** is formed by light of moderate power. Experiment have shown (see below) that fluence >1 J/cm^2 is strong while the moderate one is 0.1–1 J/cm^2.

In order to elucidate the uncommon light driven electron transfer when photon fulfill Sisyphean labor pushing an electron to the hill of the potential energy we considered the simplest situation when only two electrons are embedded into the random medium. At the absence of the light each of them will move to lower energy traps hence from the other electron. This statement is not valid for open system being under action of the light wave. Electron is transported by light to higher levels preferably if they are closer to resonance conditions. Motion to higher levels implies motion towards the other electron. We calculated numerically electron–electron correlation function (probability to find electrons at the distance between R and $R + \mathrm{d}R$). It is normalized so that for uncorrelated (noninteracting) particles the function is constant. Correlation function for intensive pumping is shown in Fig. 4. Despite the Coulomb repulsion electrons prefer to stay at some finite distance. Light indeed transports electrons against the Coulomb force compensating dark mobility aligned with the force (see also [44,45]).

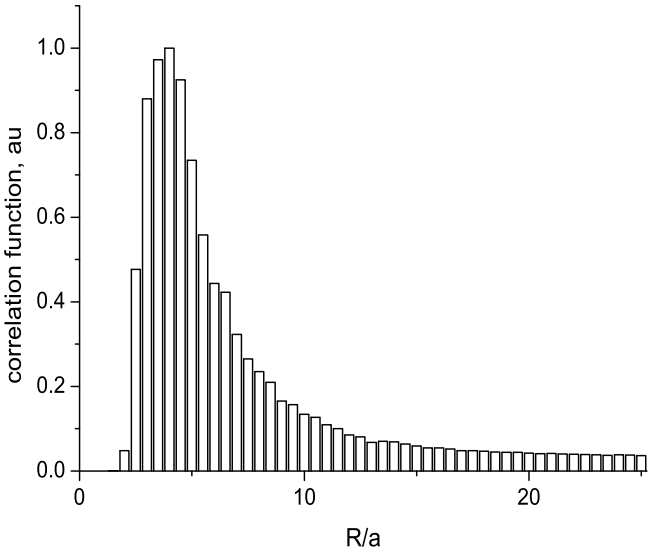

Fig. 4. Electron–electron correlation function exhibiting the light induced electron transport against the electric force $e\mathbf{E}$, a is average distance between atoms.

Many body system at moderate pumping reveals constrain connected with light polarization. The transfer rate gains maximum for the electron transport in the direction of the light polarization **e**. Other transitions are suppressed by small factor $\cos^2\theta_{fi}$ and no go during the pulse. This implies that our irradiation with **e** random in the plain perpendicular to wave number **k** transports electrons in opposite to the force direction and perpendicular to **k** as shown in Fig. 3 (starting from any trap electrons move within the plain toward the charged filament).

Our previous study of the light induced electron kinetics in random media [44,45] have shown that electron bunching takes place under intensive pumping. The induced electron charge generates strong static electric field up to 10^7 V/cm what is close to damage threshold 3×10^7 V/cm in our sample of fuzed quartz. Actions of this field upon the filament walls (strong repulsion between charged walls) splits the material analogous to crack formation. Drill deepening is accompanied by compaction effect in the walls therefore matter is not thrown from a channel. The model proposed is confirmed by the experiments presented below.

3. Experimental

High quality fused quartz samples were used in our experiments. Before the experiment the samples had been subjected to ultrasonic cleaning in acetone and ethanol

followed by washing in de-ionized water. Fragment of the experimental setup is shown in Fig. 5. The ArF excimer laser (193 nm, CL-7000, PIC GPI) was used. It generated 20 ns FWHM pulses with energies up to 350 mJ and pulse repetition rate up to 100 Hz. Laser beam was focused on the rear side of a sample by the lens made of MgF_2. Ablation has been performed in ambient air. Surface morphology and etched structures depth have been analyzed with an optical microscope with further recording with OLYMPUS C-4000 ZOOM digital camera. Normally the stable resonator for ArF laser has been used together with a homogenizer that enabled to minimize energy density distribution fluctuations (deviation from Gauss form is less than 2×10^{-2}) and also minimize spatial coherence of the beam. In some particular cases the unstable resonator has been used with the spatial coherence length not less than 6 mm in one directions – horizontal – of the beam cross-section and less than 10 μm in vertical direction.

We observed the material sputtering (ablation) on the rear side of sample produced by convergent beam with no stimulation of the process (such as plasma generation in the vicinity of a sample or specific UV absorbing medium used in [53]). The process starts itself at the upper threshold laser fluence level ≈5.5–6 J/cm^2. If the ablation threshold is passed and the polished surface is broken the process may be proceeded at lower laser fluences down to 1.5 J/cm^2.

The processed surface morphology was discussed in details in our previous papers [44,45]. We observed periodic bubble structure spaced at 2 ± 0.2 μm produced by light. The profile of the ablated crater bottom consists of packed system of half spheres ordered on the surface. The order is seen by eye and is confirmed by corresponding diffracted signal of probe HeNe beam. It is interesting that the virgin place of the sample surface near the crater is packed by the same spheres. This means that balls with fixed diameter 2 ± 0.2 μm are cut from the sample by light beam and thrown out.

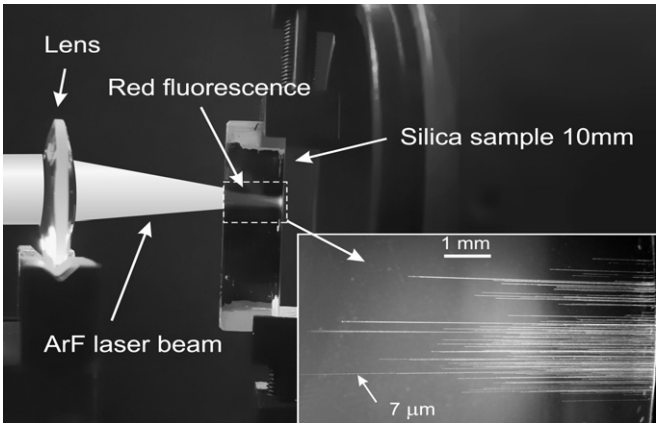

Fig. 5. Fragment of experimental setup and photo of the produced drills. Average fluence is 0.5 J/cm^2, 40,000 pulses.

The decreased light power can not support the ablation process and the ablation crater stops growing. Nevertheless another interesting phenomenon was observed at moderate fluence 0.1–1 J/cm^2 below the ablation range 1–6 J/cm^2. We observed growing of long (about 1 cm) drills aligned with **k** shown in Fig. 5. An interesting peculiarity of the channel formation is the absence of the plume: the matter is not thrown from the drills but their walls become more dense (compaction or densification effect reported by numerous authors cited above, see for example [18,29]). We monitored carefully processes in the treated sample by the digital camera. Within the ablation range fluence 1–6 J/cm^2 plume formation was recorded and corresponding fragments of the sample which are thrown out the ablation crater were studied [54]. The same procedure does not reveal plume at moderate fluence 0.1–1 J/cm^2 nevertheless drilling takes place.

We believe the drilling goes according to the following scenario. Process is triggered on the output surface where light power is maximal and electron–electron interaction is amplified by image forces. They raises near a surface and are formal way to calculate electrostatic interaction between electrons in half space. In [55] is shown that interaction in half space looks like interaction in infinite sample but an electron feels not only the other electron but also its image in symmetric position with respect to the surface. Its charge is

$$e_i = \frac{\epsilon_1 - \epsilon_2}{\epsilon_1 + \epsilon_2} e$$

where ϵ_1, ϵ_2 are dielectric constants of the sample and covering half space respectively, e is the electron charge. In our case $\epsilon_2 = 1, \epsilon_1 > 1$ and image charge has the same sign increasing the electron–electron interaction near the surface. If $\epsilon_1 < \epsilon_2$ image charge has opposite sign and the interaction is decreased. For metal cover $|\epsilon_2| \gg 1$ therefore $e_i = -e$ and electron interacts with fictitious dipole near the surface. Light transports an electron towards another electron(against the electric force) forming initial electron surface bunch. At moderate light power it grows against **k**: electron transfer goes within the plane perpendicular to **k** and against the projection of the electric force generated by the charge available (Fig. 3). Long charged filaments is produced and strong repulsion between the filament walls splits material analogous to crack formation in a stressed sample.

Drill formation needs some dose of the irradiation therefore weak pumping produces the channel during long time exposure: fluence ≈0.5 J/cm^2 about 1 h drills long channel ≈1 cm. Weak light strongly changes ground state because there are long lived excited states in glasses. These are long distant electron–hole pairs. They may be populated by weak irradiation effectively. Namely these state survive after switching off the pumping [50,51] and denote parameters of the prepared state.

We examined a lot of snaps and found that there is minimum of the drill diameters equaled 2 μm. This drill pre-

pared under fluence 0.5 J/cm^2 during 40,000 pulses is shown on Fig. 6. There are no more narrow channels and at moderate pumping one can find only these drills and their bunching therefore we shall call the narrowest channel as elemental drill. Photo under transmitted light reveals bubble structure of the elemental drill and the diameter of the blobs is also 2 μm. Increase of the light power results in bunching of the elemental drills and growing of their total cross-section. In the range of the ablation fluences 1–6 J/cm^2 this bunch becomes an ablation crater and its diameter coincides with focused spot size. At fluence >6 J/cm^2 uncontrolled cracking is observed. Fluence <0.1 J/cm^2 below the lower limit of the moderate intensity needs unreasonable long exposure to produce visible change in the fuzed quartz. Different types of the drills observed at different conditions are presented on Fig. 7. They are prepared at different fluences in the range 0.5–1 J/cm^2. Drill diameter equals to 2 μm at lower limit 0.5 J/cm^2. It increases with pumping and tends to the beam spot diameter near upper limit 1 J/cm^2. Detailed photo shows some structure of the drill walls.

New spatial scale 2 μm was observed in the other phenomena of the same family: period of the spatially ordered system of half-spheres and their diameters observed on the ablation crater bottom ([44,45]) as well as diameter of the macroscopic balls carved and thrown out the ablation crater are also 2 μm. This scale is far from the light parameters: it is three order of magnitude less than spot size (few millimeters) and one order of magnitude longer than the wavelength 193 nm used. New scale is determined by internal properties of the material (electron density mainly) what is peculiar feature of the self-organized systems. Numerous investigations of the fuzed quartz by femtosecond pulses show ordering with spatial period $\lambda/2$. Plasma is generated at this conditions and new scale is explained by interference of plasmon with light. In contrast with self-organization discussed external light parameter – wavelength λ – determines spatial scale in this case. Light intensity in our experiment due to long pulses (20 ns) was five order of magnitude less than that in femtosecond investigations what is far from the plasma generation regime and mechanism of ordering is connected with uncommon light driven electron transport in glasses. This difference in light intensities in *ns* and *fs* experiments means that nonlinear beam perturbation is negligible in our case while in *fs* study nonlinearity may be responsible for self-focusing.

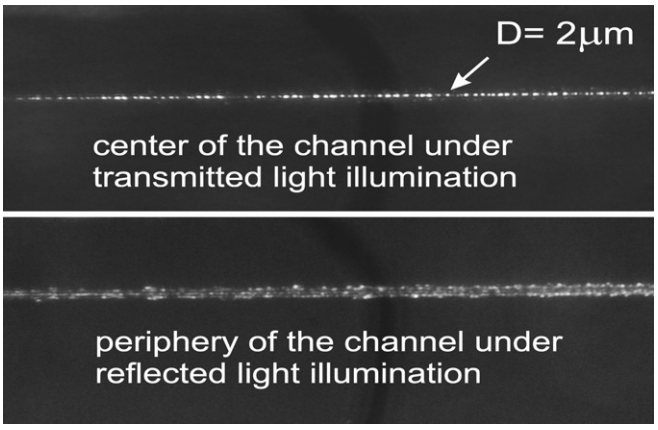

Fig. 6. Bubble structure of the elemental drill "e" shown on Fig. 7.

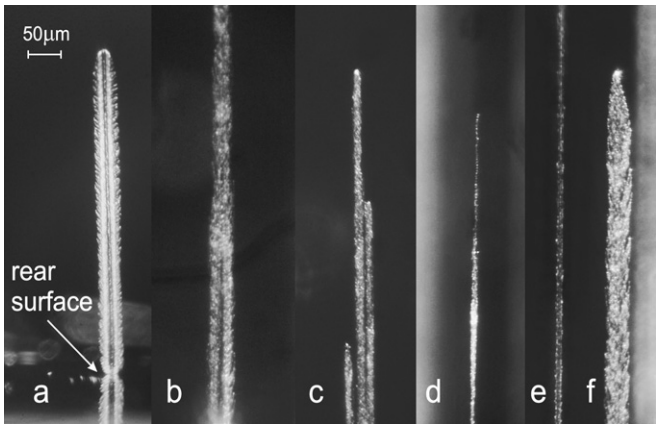

Fig. 7. Different types of the drills produced inside the sample of fused quartz. Average fluence is 0.5 J/cm^2, 40,000 pulses.

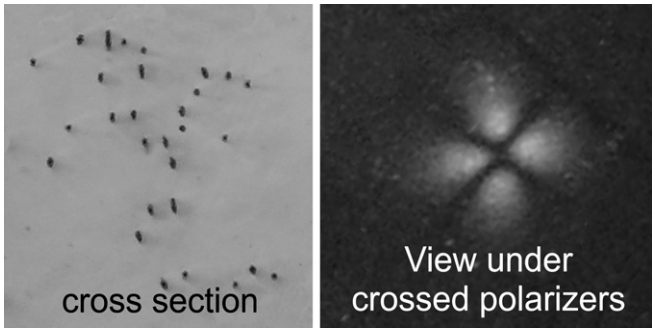

Fig. 8. Starts of the drills on the rear surface (left). The same region observed under crossed polarizers (HeNe-laser) manifested light induced birefringence (right).

Self-focusing is bright single-pulse effect: beam convergence inside a sample is followed by divergence outside easily seen at far distance. We never attained self-focusing conditions in the region of the intensities used $\approx 10^9$W/cm^2 and beam passed through the sample was not perturbed. Critical intensity is unknown for our sample but definitely it is much higher than 10^9 W/cm^2. Drill preparation is storage effect: single pulse does not produce visible change and only 4×10^4 pulses prepare long drill. Thus drill formation is not connected with self-focusing.

Output of the drills on the rear surface is shown on Fig. 8. View under crossed polarizer reveals the light induced birefringence studied in details recently (see for example [29]).

4. Conclusion

Unusual drilling of fuzed quartz by ArF laser beam was observed. Diameter of the drills are much less than the

focused spot size and material is not thrown out. According to the model proposed light produces long charged filaments aligned with wave vector **k** and their electric field (strong repulsion between the filament walls) splits the material.

Acknowledgement

This work was performed under auspices of Russian Academy of Sciences in the frame of the program "Optical spectroscopy and frequency standards".

References

[1] W. Primak, R. Kampwirth, J. Appl. Phys. 39 (1968) 5651.
[2] W. Primak, R. Kampwirth, J. Appl. Phys. 39 (1968) 6010.
[3] F.L. Galeener, J. Non-Cryst. Solids 149 (1992) 27.
[4] J.A. Ruller, E.J. Friebele, J. Non- Cryst. Solids 136 (1991) 163.
[5] J.E. Shelby, J. Appl. Phys. 51 (1980) 2561.
[6] J.E. Shelby, J. Appl. Phys. 50 (1979) 3702.
[7] P.L. Higby, E.J. Friebele, C.M. Shaw, M. Rajaram, E.K. Graham, D.L. Kinser, E.G. Wolff, J. Am. Ceram. Soc. 71 (1988) 796.
[8] E.J. Friebele, P.L. Higby, in: H.H. Bennett, A.H. Guenther, D. Milam, B.E. Newnam, M.J. Soileau (Eds.), Laser Induced Damage in Optical Materials, 1987 NIST Spec. Pub. 756, (NIST, Boulder, CO, 1988), p. 89.
[9] M. Rajaram, T. Tsai, E.J. Friebele, Adv. Ceram. Mater. 3 (6) (1988) 598.
[10] C.I. Merzbacher, E.J. Friebele, J.A. Ruller, P. Matic, Proc. SPIE 1533 (1991) 222.
[11] T.A. Dellin, D.A. Tichenor, E.H. Barsis, J. Appl. Phys. 48 (1977) 1131.
[12] C.B. Norris, E.P. EerNisse, J. Appl. Phys. 45 (1974) 3876.
[13] J.B. Bates, R.W. Hendricks, L.B. Shaffer, J.B. Bates, R.W. Hendricks, L.B. Shaffer, J. Chem. Phys. 61 (1974) 4163.
[14] W. Primak, Phys. Rev. 110 (1958) 1240.
[15] H. Sugiura, K. Kondo, A. Sawaoka, J. Appl. Phys. 52 (1981) 3375.
[16] H. Sugiura, R. Ikeda, K. Kondo, T. Yamadaya, J. Appl. Phys. 81 (1997) 1651.
[17] A. Kubota, M.J. Caturla, J. Stolken, M. Feit, Opt. Express 8 (2001) 611.
[18] M. Rothschild, D.J. Erlich, D.C. Schaver, Appl. Phys. Lett. 55 (1989) 1276.
[19] T.E. Tsai, D.L. Griscom, Phys. Rev. Lett. 67 (1991) 2517.
[20] D.L. Griscom, J. Ceram. Soc. Jpn. 99 (1991) 923.
[21] N. Kitamura, Y. Toguchi, S. Funo, H. Yamashita, M. Kinoshita, J. Non-Cryst. Solids 159 (1993) 241.
[22] R. Schenker, P. Schermerhorn, W.G. Oldham, J. Vac. Sci. Technol. B 12 (1994) 3275.
[23] R. Schenker, L. Eichner, H. Vaidya, S. Vaidya, P. Schermerhorn, D. Fladd, W.G. Oldham, in: H.E. Bennett, A.H. Guenther, M.R. Kozlowski, B.E. Newnam, M.J. Soileau (Eds.), Laser-Induced Damage in Optical Materials, Proceedings of the SPIE 2428, 1995, p. 458.
[24] R. Schenker, F. Piao, W.G. Oldham, Proc. SPIE 2726 (1996) 698.
[25] R. Schenker, W. Oldham, J. Vac. Sci. Technol. B 14 (1996) 3709.
[26] R.E. Schenker, W.G. Oldham, J. Appl. Phys. 82 (1997) 1065.
[27] D.C. Allan, C. Smith, N.F. Borrelli, T.P. Seward, Opt. Lett. 21 (1996) 1960.
[28] K.M. Davis, K. Miura, N. Sugimoto, K. Hirao, Opt. Lett. 21 (1996) 1729.
[29] N.F. Borrelli, C. Smith, D.C. Allan, T.P. Seward, J. Opt. Soc. Am. B 14 (1997) 1606.
[30] L. Skuja, J. Non-Cryst. Solids 239 (1998) 16.
[31] E.M. Wright, M. Mansuripur, V. Liberman, K. Bates, Appl. Opt. 38 (1999) 5785.
[32] V. Liberman, M.R. Rothschild, J.H.C. Sedlacek, R.S. Uttaro, A. Grenville, J. Non-Cryst. Solids 244 (1999) 159.
[33] N.F. Borrelli, C. Smith, D.C. Allan, T.P. Seward, Opt. Lett. 24 (1999) 1401.
[34] P.R. Herman, K.P. Chen, P. Corkum, A. Naumov, S. Ng, J. Zhang, SPIE Proc. 4088 (2000) 345.
[35] F. Piao, W.G. Oldham, E.E. Haller, J. Non-Cryst. Solids 276 (2000) 61.
[36] Y. Ikuta, K. Kajihara, M. Hirano, S. Kikugawa, H. Hosono, Appl. Phys. Lett. 80 (2002) 3916.
[37] J. Zhang, P. Herman, C. Lauer, K. Chen, M. Wei, Proc. SPIE 4274 (2001) 125.
[38] Y. Ikuta, S. Kikugawa, M. Hirano, H. Hosono, J. Vac. Sci. Technol. B 18 (2000) 2891.
[39] Y. Ikuta, K. Kajihara, M. Hirano, H. Hosono, Appl. Opt. 43 (2004) 2332.
[40] K. Kajihara, Y. Ikuta, M. Hirano, H. Hosono, Opt. Lett. 81 (2002) 3164.
[41] A. Zoubir, M. Richardson, L. Canioni, A. Brocas, L. Sarger, J. Opt. Soc. Am. B 22 (2005) 2138.
[42] S.O. Kucheyev, S.G. Demos, Appl. Phys. Lett. 82 (2003) 3230.
[43] M.A. Stevens-Kalceff, A. Stesmans, Joe Wong, Appl. Phys. Lett. 80 (2002) 758.
[44] B.P. Antonyuk, V.B. Antonyuk, A.Z. Obidin, S.K. Vartapetov, M.A. Kurzanov, Opt. Commun. 230 (2004) 151.
[45] B.P. Antonyuk, A.Z. Obidin, K.E. Lapshin, Phys. Lett. A 332 (2004) 86.
[46] H. Benard, Rev. Gen. Sci. Pures Appl. 12 (1900) 1261.
[47] A.N. Zaikin, A.M. Zhabotinsky, Nature 225 (1970) 535.
[48] A.M. Turing, Phil. Trans. R. Soc. London B 237 (1952) 37.
[49] F.T. Arecchi, Physica D 86 (1995) 297.
[50] B.P. Antonyuk, V.B. Antonyuk, Physics-Uspekhi 44 (2001) 53.
[51] B.P. Antonyuk, Light Driven Self-Organization, Nova Science Publishers, Inc., NY, 2003.
[52] R. Kubo, Y. Toyazawa, Progr. Theor. Phys. 13 (1955) 160.
[53] K. Sugioka, J. Zhang, K. Midorikawa, Laser Machining Method and Laser Machining Apparatus, Patent No.: US 6 180 915 B1, 2001.
[54] B.P. Antonyuk, A.Z. Obidin, K.E. Lapshin, S.K. Vartapetov, Opt. Commun. 281 (2008) 191.
[55] L.D. Landau, E.M. Lifshitz, L.P. Pitaevskii, Electrodynamics of Continuous Media, Pergamon Press, Oxford, 1984.